COMBINED LIGHT/HEAT/GAS SENSORS WITH DECOUPLED ELECTRICAL AND THERMAL RESISTANCES

A. Y. Kovalgin, J. Holleman, A. van den Berg

MESA+ Research Institute, University of Twente
P.O. Box 217, 7500 AE Enschede, The Netherlands.
Phone: +31-53-4892841 Fax: +31-53-4891034
E-mail: A.Y.Kovalgin@el.utwente.nl

***Abstract* – This work extends our previously reported idea of maintaining a hot surface by means of dissipating power at a nano-scale conductive link (antifuse). Two approaches to the device design are considered: the hot surface can be either reduced to a sub-µm-size hotspot or maintained within a larger diameter of a few microns. The designs have an advantage of decoupling the electrical resistance and thermal resistance of the device.**

This paper contains the results of theoretical modelling and practical realization of the antifuse-based devices. The so-called pillar-shape antifuses have been practically realised and measured. The sensitivity to different sources of energy and thermo-electrical properties have been investigated. It appeared that a pillar-shape antifuse could perform as a combined nano-scale heat detector and light sensor. Furthermore, because of the ability to generate heat, we have studied the use of the pillar-shape antifuses for vapour sensing. First promising results showed a high response after introducing acetone (ethanol) vapour into the measuring chamber. No catalytic layer aiming at decreasing the operating temperature and increasing the sensitivity was deposited on the device surface.

***Keywords* – gas sensor, light sensor, heat sensor; nano-hotspot; antifuse**

I. INTRODUCTION

Hot-surface devices have received much attention nowadays because of their utilization for Pellistor-type gas sensors [1] and micro reactors. This work employs the idea of maintaining a hot surface by means of antifuses [2]. The antifuses can maintain a non-uniform hot surface within a diameter of a few µm at very low power consumption [3]. The devices can also be designed in such a way that the hot surface area is reduced to a sub-µm-size hotspot [4].

Apart from the low power consumption, the advantage of the proposed concept is *decoupling the electrical resistance and thermal resistance*. For conventional hot plate devices, a high thermal resistance of the leads is needed to minimize the power losses. This can only be achieved by shrinking the cross-sections, which results in a higher electrical resistance and undesired extra power dissipation. In our approach, the devices are designed in such a way that one can manipulate the heat flow without affecting the electrical resistance.

In this paper, we demonstrate our results with respect to design, modelling, practical realisation and experimental characterisation of the combined light/heat/gas sensors employing the antifuse concept.

II. DESIGN

The antifuse-based approach is realised in two structures (Fig 1). For ***Structure 1***, the hot surface is thermally isolated from the bottom silicon electrode only by means of a 500-nm LOCOS oxide (Fig 1a). This ensures a reduced hot area needed for scanning/probing technique. The attention is paid to pre-determination of the link location on the surface. To improve the feasibility of the device as a Pellistor-type gas sensor, ***Structure 2*** with improved thermal isolation for maintaining a larger hot area has been proposed (Fig 1b).

Already fabricated *Structure 1* consists of two electrodes: rather thick mono-Si pillar-type bottom electrode and very thin poly-Si top electrode (passivated). The surrounding oxide plays an important role for thermo-electrical isolation and confines the area of antifuse formation. The process flow employs standard LOCOS oxidation and CVD technology [4, 5]. In still not realized practically *Structure 2*, both electrodes are designed from thin poly-Si layers. The suspended membrane provides improved thermal isolation. No steps towards pre-determined-in-space antifuse formation are yet made.

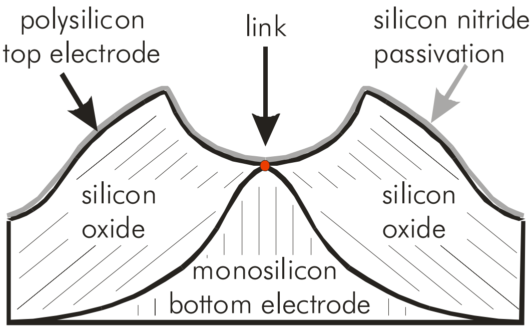

a) Pillar-shape device (Structure 1)

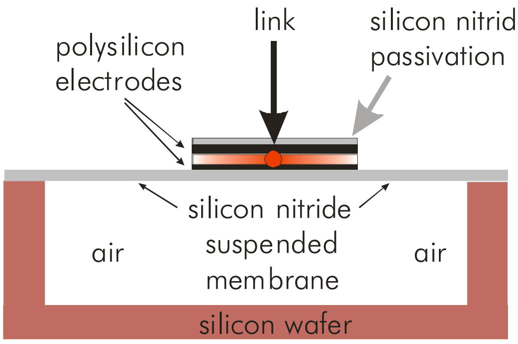

b) Suspended-membrane device (Structure 2)

Fig 1. *Schematics of the proposed structures.*

III. MODELLING

Fig 2 represents modelled surface-temperature gradients for *Structure 1* and *Structure 2*. For *Structure 1*, a link of 10 nm in diameter can maintain a very sharp temperature profile at power consumption in the range of mW. For *Structure 2*, equivalent in size link provides smoother temperature distribution at similar powers. Modelled temperature profiles exhibit the possibility to induce thermo-chemical reactions on micro-scale.

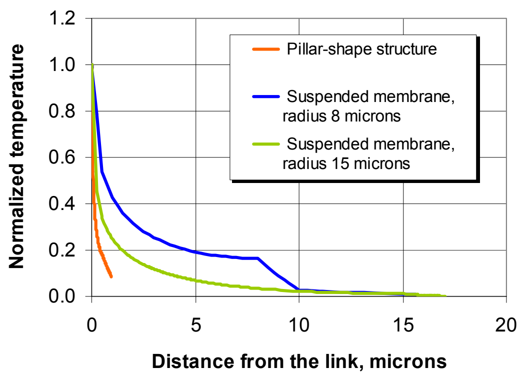

Fig 2. *Temperature gradients for a 10-nm link (modelled with SILVACO's ATLAS).*

An important characteristic is the power density per unit surface area, needed to increase the surface temperature in one degree (SPDD). From modelling (Fig 3), SPDD mainly depends on two parameters: poly-Si electrode thickness and electrode diameter. It appears that SPDD gradually increases with poly-Si thickness. However, it significantly drops with increasing radius of the poly-Si plate. This is due to the competition between lateral heat transfer conditions in the poly-Si layer (which are favourable for a thicker poly) and vertical heat losses through the membrane material and air. From Fig 3, a 210-nm thick electrode with a diameter of 26 µm provides the same SPDD as a 110-nm thick electrode having a diameter of 16 microns.

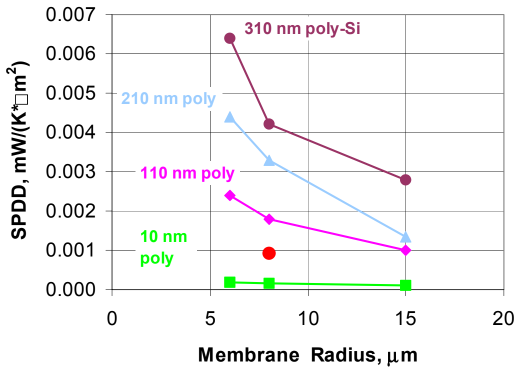

Fig 3. *Surface power density applied per one degree, (modelled for Structure 2 with SILVACO's ATLAS).*

IV. EXPERIMENTAL

A. *I-V Characteristics*

Initial electrical programming of *Structure 1* was performed accordingly to [4, 5].

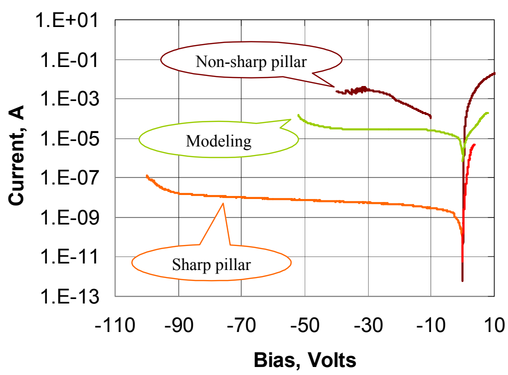

Fig 4. *I-V characteristics of the pillar-shape structure with the same doping of the electrodes.*

An important result is that a pillar-shape antifuse with the same type of electrode doping behaves similar to a diode (Fig 4). Negative biasing results in much higher device resistance compared to positive biasing. A very small link is able to keep the current as low as 0.1 µA even if –100 V is applied. The diode-like behaviour can be explained, for example, in terms of the depletion with electrons in the low-doped silicon pillar. The modelling based on the depletions effects shows the same qualitative behaviour (Fig 4). Additionally, the difference in the I-V characteristics between a sharp pillar (easier to deplete) and a non-sharp pillar (more difficult to deplete) confirms that the depletion plays a role.

B. Generation of Heat

The following experimental results exhibit the feasibility of *Structure* 1 to perform as a hot-surface device. Fig 5 represents a series of the surface images for the devices programmed at positive bias. First (a), one can notice no features on the surface of a fresh non-programmed device. Second (b), after programming at 1 mW, a round spot appears at the centre. This spot can be attributed to the conductive link. One can estimate the link diameter of about 70 nm. Third (c), after a gradual increase of power up to 4.5 mW, the surface area significantly deteriorates compared to that depicted in (b). At even higher powers, the evaporation of both the poly-Si layer and nitride film can be observed [4].

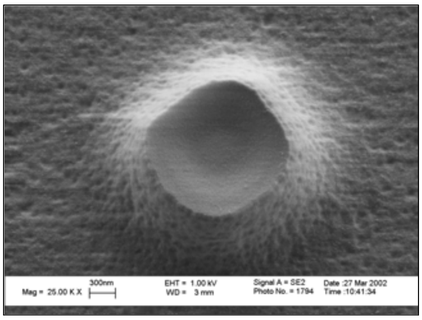

a) Before programming

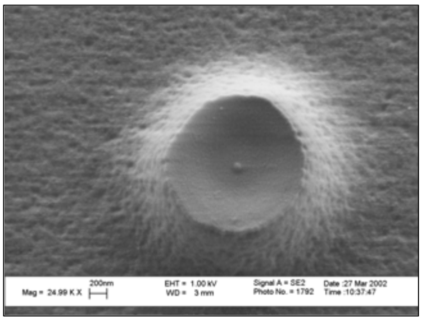

b) After programming the link at 1 mW.

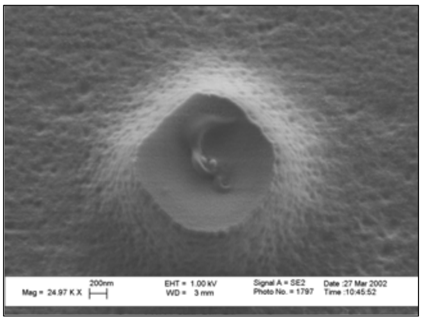

c) After programming the link at 4.5 mW.

Fig 5. *SEM image of the device after programming at different powers.*

C. Experiments on Sensitivity

Sensitivity of the pillar antifuses to different sources of energy has been investigated. It appeared that a pillar antifuse was able to perform as a combined nano-scale heat-, light-, and vapour-sensor.

The depletion can additionally cause the sensitivity of the device resistance to substrate temperature at negative biasing (Fig 6). Namely, due to a low concentration of free carriers in the close-to-link area of the sharp silicon pillar the pillar resistance becomes a sensitive measure of temperature. The extra heat supplies new carriers, which leads to the resistance drop.

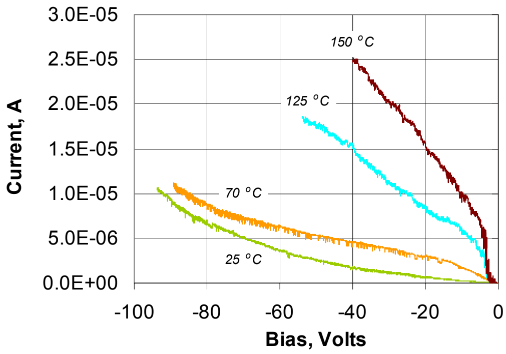

Fig 6. *I-V characteristics of pillar antifuses at different substrate temperatures; bias is applied to poly-Si electrode.*

The same matters causing sensitivity to heat can also result in a dramatic drop of the resistance during illumination with light (Fig 7). As expected, sensitivity to light decreases with increasing temperature. This is due to the fact that both heat and light provide extra carriers and, therefore, can independently suppress the depletion effects. In Fig 7, one can notice that the response to light is hard to measure if the temperature exceeds 125 ^{o}C.

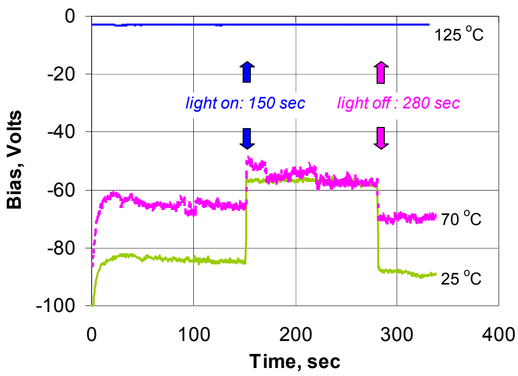

Fig 7. *Sensitivity to light at different substrate temperatures during a constant current stress of –100 nA, bias is applied to poly-Si electrode.*

Because of the ability to generate and detect heat, the pillar-shape structure seems to be appropriate for vapour sensing. First promising results have already been obtained in this direction. In Fig 8, one can observe a significant response after introducing acetone vapour into the measuring chamber. Fig 9 shows less response to ethanol. It is important to bear in mind that no catalytic layer aiming at decreasing the operating temperature and increasing the sensitivity was deposited on the device surface.

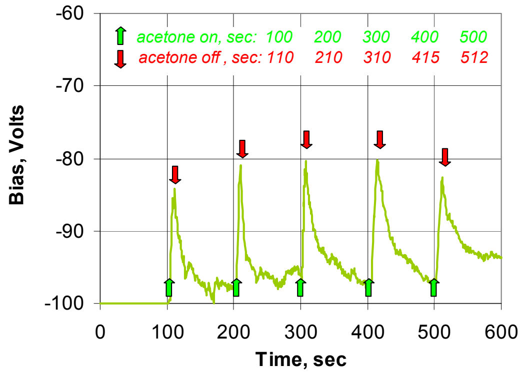

Fig 8. *First experiments on sensing of acetone vapour; a low power of 95 micro Watt is applied.*

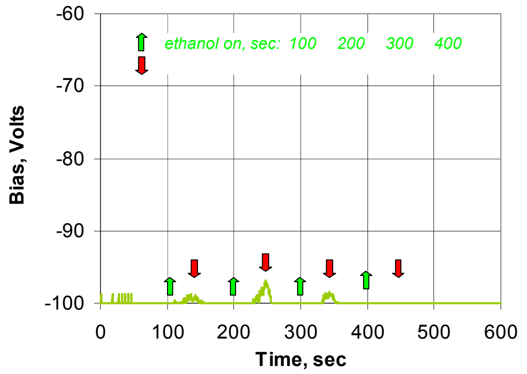

Fig 9. *First experiments on sensing of ethanol vapour; a low power of 100 micro Watt is applied.*

D. Re-programming and reliability issues

Once realized I-V characteristics can be multiply repeated, provided that the programming parameters (current, power, etc.) are not exceeded. Exceeding the programming values causes re-programming of the link, which results in the rather noisy behaviour (Fig 10). The link resistance can become lower or higher after re-programming depending on the re-programming conditions. A resistance drop can be attributed to gradual enlarging the link due to its re-melting. An increase of the resistance can be explained in terms of an irreversible change in the material quality (diffusion, charge transfer, etc.). High temperatures or high electric fields can provide this change.

Stability tests have been carried out for some of the fabricated devices. The attention was paid to the stability during applying a negative bias to the poly-Si electrode. This was important because the devices show no sensitivity at positive bias. For the stability tests, the antifuses were first programmed at -1 μA (power of ~100 μW) and then kept under a fixed current of -1 μA for several hours (up to several days). It appears that instability during the first hours can be observed, followed by reasonably stable behaviour. However, since the devices still show good sensitivity at much lower currents/powers, we expect only minor instabilities at the operating conditions.

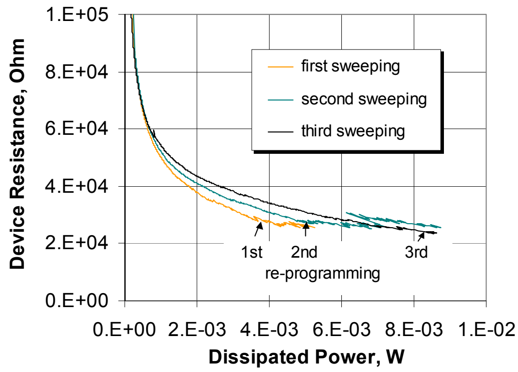

Fig 10. *Measured antifuse resistance versus applied power; the re-programming acts can clearly be seen.*

V. Conclusions

In this work, we have proposed and studied novel device structures with decoupled electrical and thermal resistances. The experimentally measured pillar-shape antifuses exhibit the feasibility to perform as combined nano-scale heat-, light-, and vapour-sensors operating at very low power consumption in the range of micro Watts.

VI. Acknowledgements

This work is financially supported by the EU project GRD1-1999-10849.

VII. References

[1] M. Gall. *Sensors and Actuators B (Chemical)* **B4**, 533-8 (1991).

[2] V. E. Houtsma, Ph.D. Dissertation, University of Twente, Enschede, The Netherlands, (1999).

[3] A. Y. Kovalgin, J. Holleman, A. van den Berg. In "*Sensor Technology 2001*", ed. M. Elwenspoek, Kluwer Academic Publishers, p. 107-112, (2001).

[4] A.Y. Kovalgin, J. Holleman, A. van den Berg. Eurosensors 2002 – Book of Abstracts (Part I, Part II, Part III), edited by J. Saneistr and P. Ripka, pp. 31-32. The four-page full paper is available in the CD-ROM proceedings, pp. 88-91.

[5] A.Y. Kovalgin, J. Holleman, A. van den Berg and H. Wallinga. STW/SeSence2001 Proceedings, pp. 809-812.